In the other word, CPS equips with an internal circuits that produce current in output. After CPS calibration, which is performed based on lower and upper pressure limits, it is expected that the output current, $I_{measured}$, to be a linear function of the input differential pressure, Δp, as:

$$I_{measured} = \alpha \Delta p + \beta, \quad (5)$$

where α and β are two parameters that should be tuned in order to achieve the minimum error in pressure measurement [10]. In many applications, $I_{measured}$ is measured by a current measurement system and then, it is converted to the input differential pressure, Δp, as:

$$\Delta p = (I_{measured} - \beta) / \alpha, \quad (6)$$

In converting the CPS output current to the input pressure using Equation (6), unfortunately, there is always an error that is based on linear approximation, which is presented in Equation (5), for nonlinear dependencies.

III. PROPOSED MLP-BASED COMPENSATION FRAMEWORK

Two main principles for MLP-based CPS compensation are characteristics of neural networks including: self-adaptive capacity, which is necessary for complicated nonlinear mapping, and training ability, which is suitable for adapting based on real data. As discussed in Section 2, the current output of a CPS is dependent on both pressure and temperature. The pressure dependency is normal for a CPS, but in the situation that CPS temperature changes, the CPS output does not indicate the exact pressure. By using the MLP neural network, the adverse effects of temperature as well as nonlinear dependencies on the CPS output is reduced and compensated. For a CPS that is equipped to MLP-based compensator, it is expected that the linear Equation (5) to be fully establish, independent of temperature variations and CPS nonlinear dependencies.

Figure 2 shows the first proposed setup for a CPS equipped with a MLP-based compensation that simulates the compensated output current, $I_{compensated}$. In this figure, the PT100 is a common calibrated temperature sensor which generates ambient temperature value, $T_{measured}$, in order to be one of the MLP input. After MLP training, it is expected that MLP output value, $I_{compensated}$, is not only temperature-invariant, but also fully linear respect to the input differential pressure, Δp, which is presented in Equation (5).

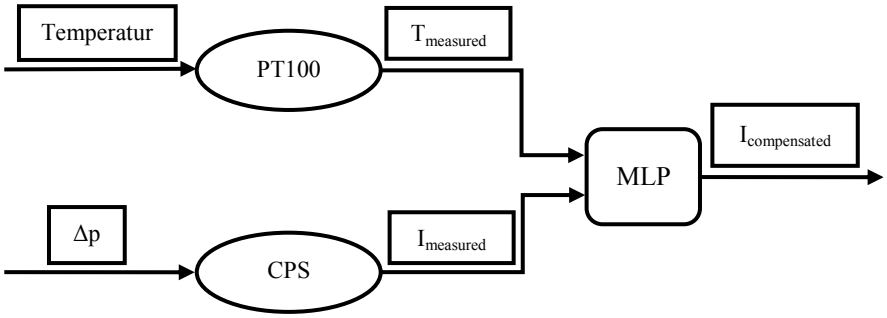

Figure 2. The first proposed setup for a CPS equipped with a MLP-based compensation which simulates the compensated output current

In the proposed framework, the MLP training plays a major role in validity of the compensator performance. Figure 4 demonstrates the proposed training setup for the MLP used in the first proposed framework which is shown in Figure 2. In this setup, it is necessary to generate the error value, which is a difference between the real output of MLP, $I_{compensated}$, and the ideal value of CPS current output, I_{ideal}, based on the Equation (5). In order to compute I_{ideal} based on the Equation (5), it is necessary to use an accurate input differential pressure, $\Delta p_{measured}$, which is measured by another calibrated and accurate pressure sensor, accurate PS, in the proposed setup which is shown in Figure 3.

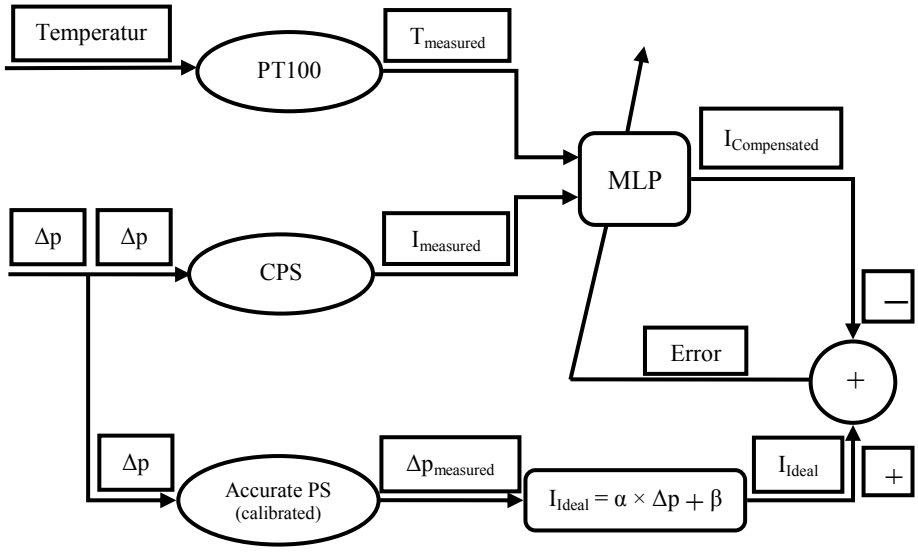

Figure 3. The proposed setup for training of MLP-based CPS compensation which simulates the compensated output current

The previous setup generates the compensated output current, while in some applications, it is necessary to generate pressure value, instead of current, in the measurement system output. So the second framework is also proposed, which is shown in Figure 4, in which the MLP output simulates $\Delta p_{measured}$.

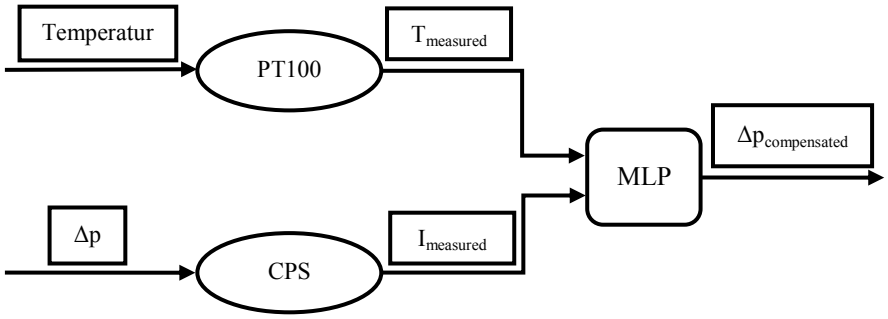

Figure 4. The second proposed setup for a CPS equipped with a MLP-based compensation which simulates the compensated pressure value

The only difference between two proposed frameworks is the MLP used in the second framework is trained to generate the compensated pressure value while in the first one the MLP is trained to generate the compensated corresponding current. Figure 5 also demonstrates the proposed training setup for the MLP used in the second proposed framework which is shown in Figure 4. In this setup, the generated error for MLP training is based on error between the generated pressure by MLP and the accurate PS which is shown in Figure 5.

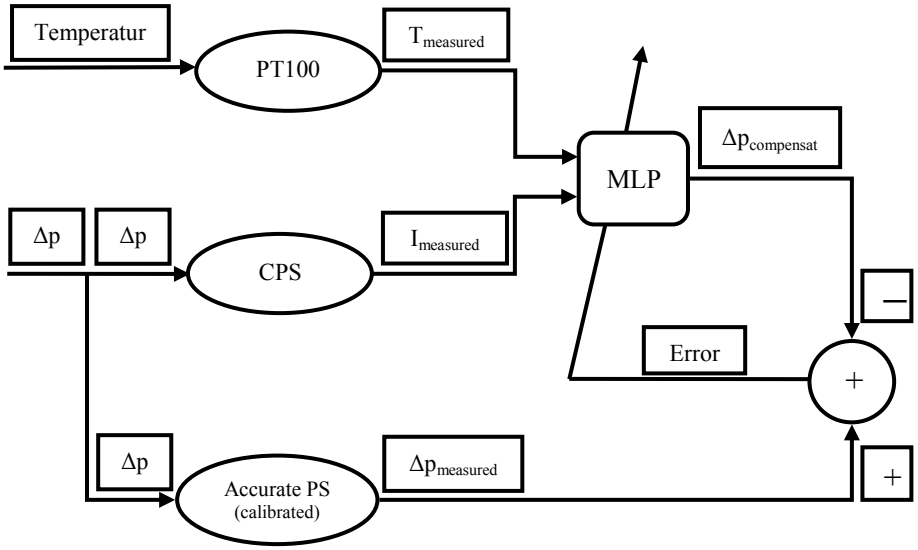

Figure 5. The proposed setup for training of MLP-based CPS compensation which simulates the compensated output current

IV. USING COMPENSATION FRAMEWORK FOR A SAMPLE CPS

This section presents realization of proposed compensation framework for eliminating the negative effects of ambient temperature as well as non-linear dependencies for the sample CPS, AUTROL® APT3100 smart pressure transmitter, which is shown in Figure 6 [14]. This sensor can be used for pressure measuring of corrosive or non-corrosive gases, water vapor and liquids. Its measurement range is between 0 mmh_2o to 3874 mmh_2o. The APT3100, which is a two wire loop power transmitter, equips with a standard 4/20mA output scaled for desired output pressure range. It is claimed that the value of the output current is the linear dependent on the input pressure sensor. This output signal can be indicated, recorded, or used in a control system.

Figure 6. AUTROL® APT3100 which is a CPS-based smart pressure transmitter

However, this smart sensor uses a capacitive pickup optimized with a patented temperature compensation algorithm, but our experimentations improve that this smart sensor still suffers from dependency to temperature. Therefore, we used our proposed framework for compensating. At the first step, it is necessary to perform some experiments on the APT3100 in different operations, in order to collect a comprehensive dataset which is needed for MLP training.

a. Collecting Data

In order to collect a comprehensive dataset, the laboratory system which is schematically shown in Figure 7, is designed to emulate real conditions in which the sensor is practically used.

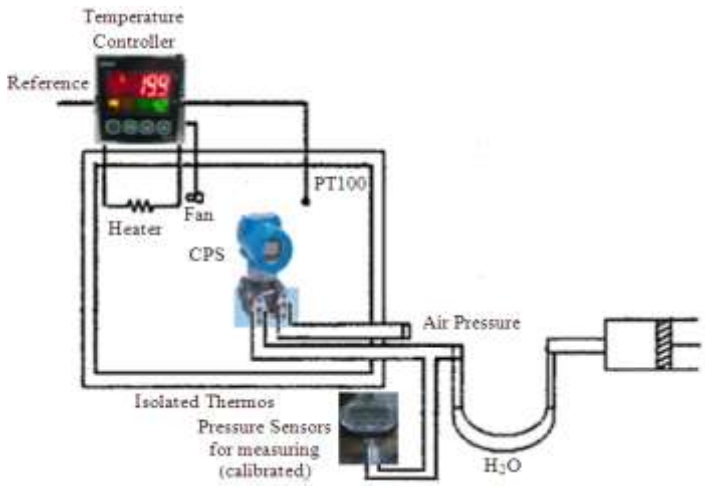

Figure 7. The schematic diagram of the proposed test system which is designed to study the effect of temperature on APT3100 output

Figure 8 also shows the built system in real environment which includes the temperature controller system, the thermal isolated container with an APT3100 and a heater inside, the other calibrated pressure sensor for accurate measuring the pressure, the handy air pump for producing different pressure, the manometer and some other parts.

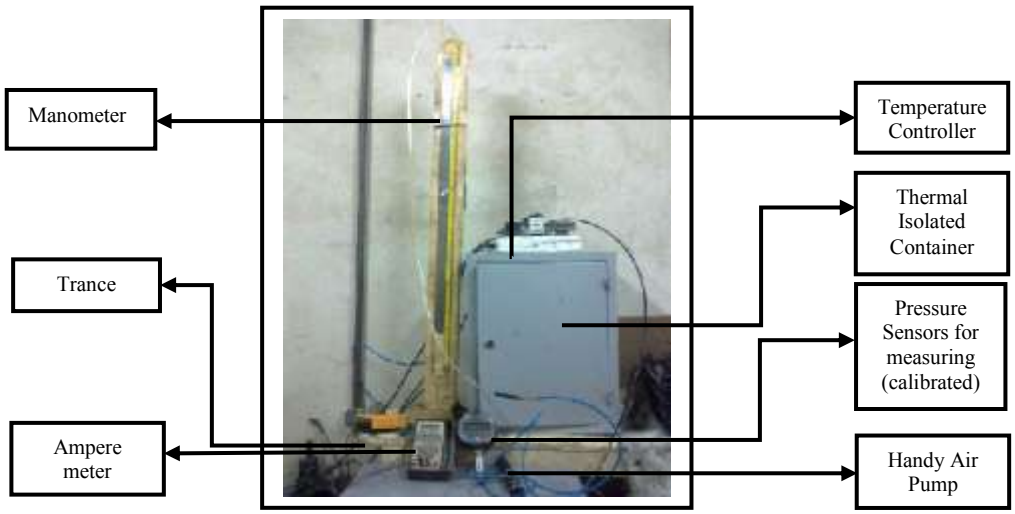

Figure 8. The real test bench used to achieve experimental data

To evaluate the effect of temperature on the behavior of ATP3100 output, the temperature inside the compartment from +5 °C to +60 °C with incremental step of 5 °C is applied. Moreover, at any particular temperature, differential pressure acts on the diaphragm of CPS from 0 mmh_2o to 500 mmh_2o with incremental step of 50 mmh_2o is applied.

Totally, 12 datasets that each of these sets contains 11 pairs of (I,Δp) are obtained, where Δp is differential input pressure which is measured by the calibrated pressure sensor (in mmh_2o unit) and I is the sensor output current which is measured by the ampere meter (in mA unit). In each dataset, the ambient temperature is fixed which means that the output current or differential pressure is independent of temperature. For example, at the first (last) dataset, the temperature is fixed on 5 (60) °C.

Before starting experiments for each dataset which is considered in a fixed temperature, it is necessary to calibrate the APT3100 for the ambient temperature. In ambient temperature, a HART device [14] or computer calibration action is used for pressures 0, +125, +250, +375, +500 mmh_2o as the sensor input, to produce 4, 8, 12, 16, 20 mA as the sensor output, respectively.

On the other hand, since a heater is used for adjusting temperature value inside the thermal isolated container, the APT3100 should be placed at that temperature for about 1.5 hours to guaranty the temperature inside the chamber capacitive diaphragm of CPS reaches to the desired temperature and the temperature impact has been completed on APT3100 output.

b. Datasets

Each dataset shows the effect of environment temperature as well as other nonlinear effects on the behavior of the sensor output. For example, Figure 9 presents a sample dataset that is the output current for every real input differential pressure, at 60 °C. The blue continuous line is ideal output while the red dashed line in the real output. Since the sensor was calibrated to produce the linear output current based on the input differential pressure (Equation 5), there is a slight deviation between the ideal and real output, which is shown in Figure 10, for the sample dataset of Figure 9.

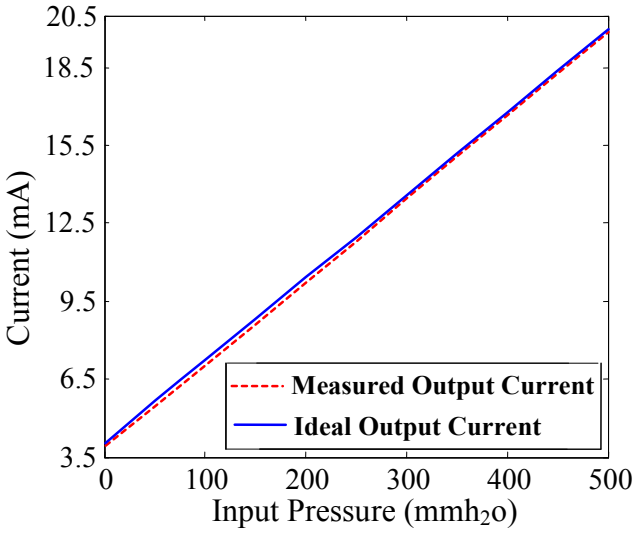

Figure 9. The sample dataset: The output current of the APT3100 versus the real input differential pressure at the tested temperature of 60 °C

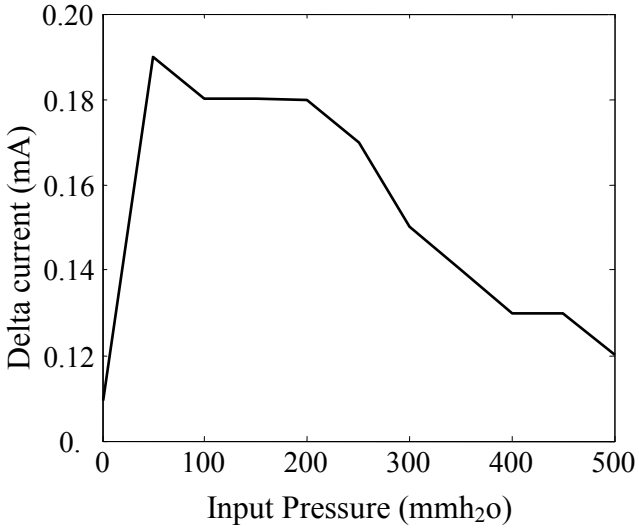

Figure 10. The sample difference between the ideal and real output current of the ATP3100 versus different real input differential pressure, at 60 °C

On the other hand, the output current can be used to compute the input differential pressure (by Equation 6) that results in a slight deviation between the real and the measured input differential pressure which is shown in Figure 11, for the sample dataset of Figure 9.

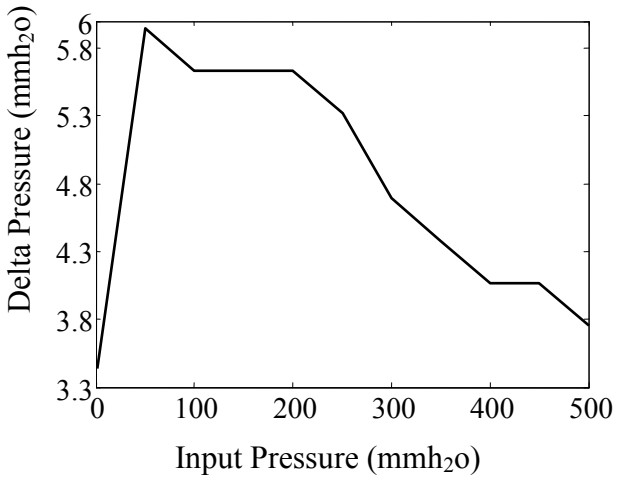

Figure 11. The sample for difference between the real and the measured input differential pressure of the ATP3100 versus different real input differential pressure, at 60 °C

Figures 9 through 11 present the nonlinear effects which results in a slight difference between real and desired values. For example, Figure 11 shows there are 3.3 to 6 mmh_2o differences between the real and measured input differential pressures. Again, the datasets can be used to present the dependency of the output values to the APT3100 real temperatures. For example, Figure 12 shows the APT3100 output current for fixed input differential pressure 500 mmh_2o which should be 20 mA, in different temperatures.

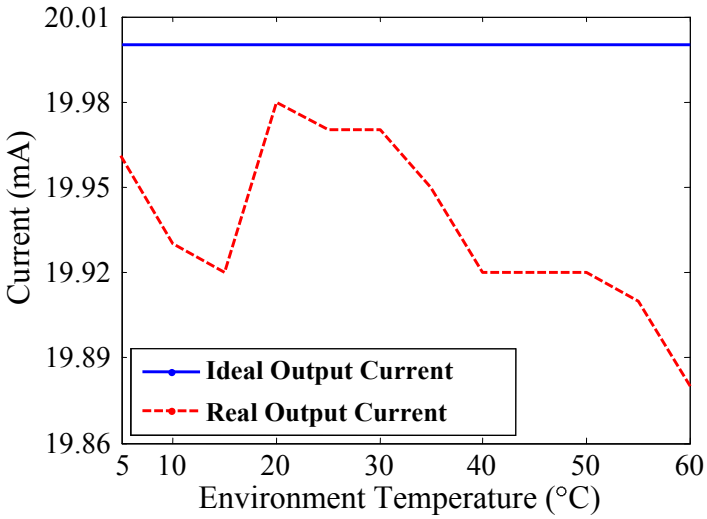

Figure 12. The samples for difference between the ideal and real output current of the ATP3100 for the fixed input differential pressure of 500 mmh_2o versus different environment temperatures

Figure 13 also shows the computed input differential pressure of the APT3100 based on the corresponding output current for fixed input differential pressure 500 mmh_2o in different temperatures. There are some noticeable differences between the real and measured input differential pressure. Figures 10 and 13 demonstrate the nonlinear effects as well as temperature impacts on the measured input differential pressure. It means that it is necessary to consider the other compensating system to reduce these effects in order to produce perfect output.

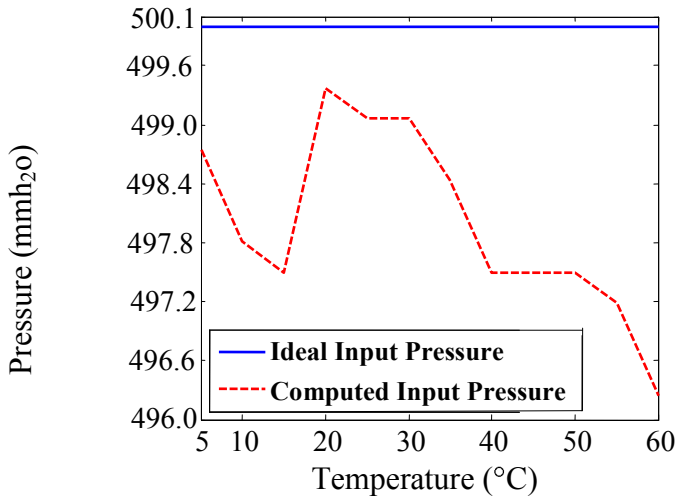

Figure 13. The sample for difference between the real and the measured input differential pressure of 500 mmh_2o based on the output current of the ATP3100 versus different environment temperatures

c. Applying Compensating Framework

One of the main parts of the compensating framework is MLP neural networks that should be train accurately for perfect working. Therefore to consider the proposed compensating framework in the testing system, a training set based on the collected datasets should be used for MLP training. The training set should be divided into two sets: training and testing. During the training phase, the training dataset is used for MLP training by different learning algorithms [13,15-17], until achieving to a predefined error, between desired and real outputs. In the testing phase, the testing dataset is applied to the trained MLP to compute error for testing dataset. If there are different MLP architectures and different learning algorithms, the best MLP achieves to the lowest testing error.

The datasets consist of a collection of triple data (I,T,Δp), where I is the measured output current. The temperature (T) includes 12 different values from 5 to 60 °C with incremental

temperature step of 5 °C. The input differential pressure (Δp) includes 11 different values from 0 to 500 mmh_2o with incremental pressure step of 50 mmh_2o. Therefore the total dataset consists of 132 (12×11) triple data (I,T,Δp) which is divided into two sets, 2/3 of data is selected for training, and 1/3 of the remained data is selected for testing. The total data for temperatures values of 5, 10, 20, 25, 35, 40, 50, and 55 °C are assigned for training, and the other data for temperatures values of 15, 30, 45, and 60 °C are assigned for testing.

The evaluated MLPs are two and three layers with different number of neurons in the hidden layers. These MLPs have two inputs and one output which are shown in Figures 2 and 4. For two layers MLP, the number of neurons in the hidden layer is selected between 1 to 20 neurons, while for the three layer MLP, the number of neurons in the second hidden layer is selected between 1 to 10 neurons. Different excitation functions including linear, sigmoid, hyperbolic tangent and logarithmic functions are tested. Moreover, different learning algorithms are used for MLP training including Batch Backpropagation, Batch Backpropagation plus Momentum, Resilient Propagation, Quasi-Newton and Levenberg-Marquardt algorithms. The training and testing procedures are repeated 10 times from different initial MLP weights, and the average output values are computed and considered.

d. Simulation Results

Our simulations show that the best neural network is the three layers MLP with 6 and 4 neurons in the first and the second hidden layer, respectively. The excitation function in the output layer is linear while in the other layers, hyperbolic tangent is used. Moreover, the Levenberg-Marquardt (LM) learning algorithm presents the lowest testing error. Figure 14 compares the results of applying the trained MLP-based compensating system for dataset shown in Figure 9.

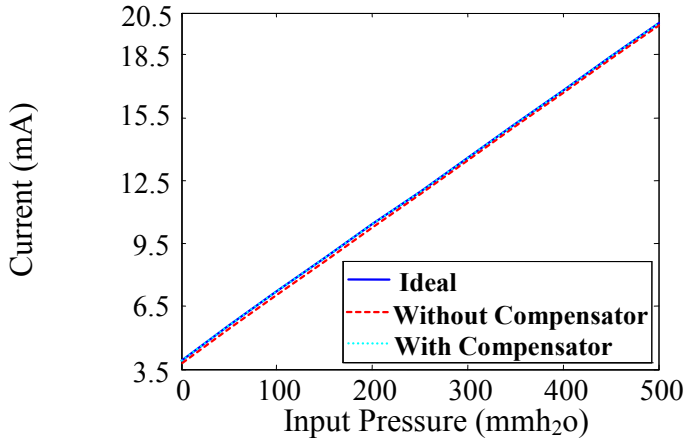

Figure 14. The output current of the APT3100 versus the real input differential pressure at the tested temperature of 60 °C, for three cases: ideal output, with and without applying MLP-based compensator.

In order to highlight the difference between the APT3100 current output before and after applying the trained MLP-based compensating system, Figure 15 shows the difference between the ideal output current with these two cases. It is clear that the deviation is effectively reduced using the proposed MLP-based compensating system.

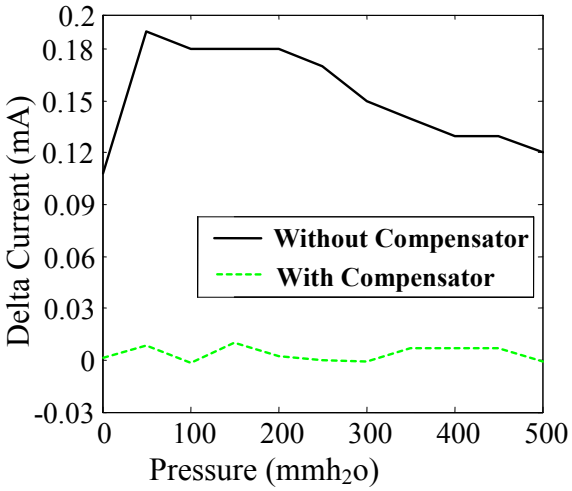

Figure 15. The sample difference between the ideal and real output current of the ATP3100 versus different real input differential pressure, at 60 °C, for two cases: with and without using MLP-based compensator system.

As discussed before, ATP3100 can be used to compute the input differential pressure based on the measure output current. Figure 16 demonstrates the difference between computation of

the input differential pressure in two cases, with and without using the MLP-based compensating system, at the fixed temperature 60 °C, where the error effectively reduces when the proposed compensator is used.

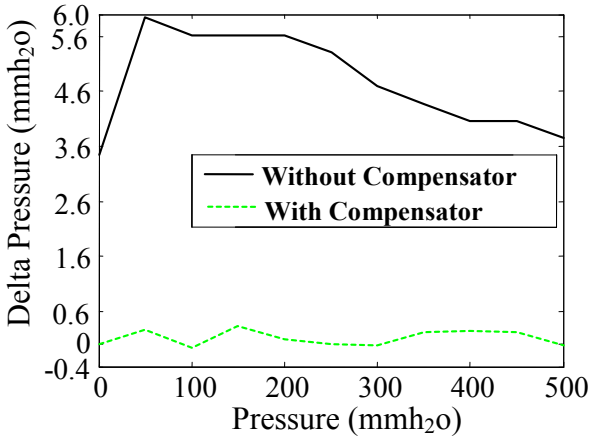

Figure 16. The sample for difference between the real and the measured input differential pressure of the ATP3100 versus different real input differential pressure, at 60 °C, in two cases: with and without applying the trained MLP-based compensating system.

In order to present effectiveness of the trained MLP-based compensating system in different environment temperature, Figure 18 and 19 show the output current and the computed input differential pressure, respectively, in different temperature, at pressure of 500 mmh_2o. The output compensated current in Figure 18 is very close to 20 mA which is the ideal output current. Moreover, the computed pressure by the compensated system is very close to 500 mmh_2o which is the input differential pressure.

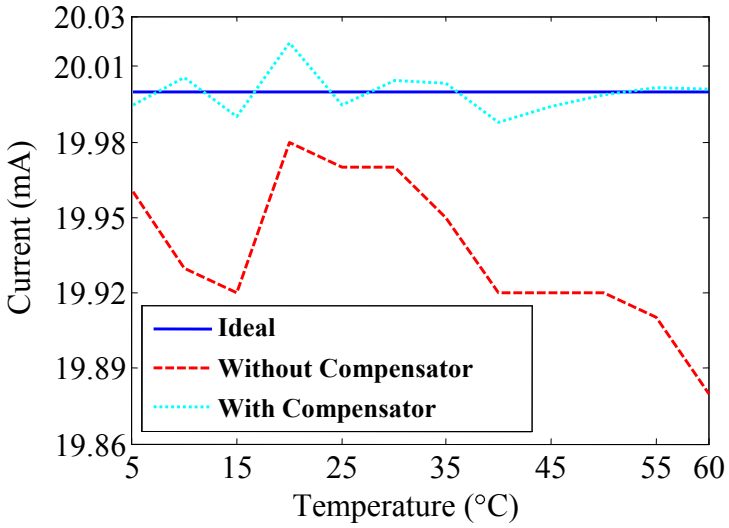

Figure 17. Comaprison between the ideal, real and compensated output current of the ATP3100 for the fixed input differential pressure of 500 mmh_2o versus different environment temperatures

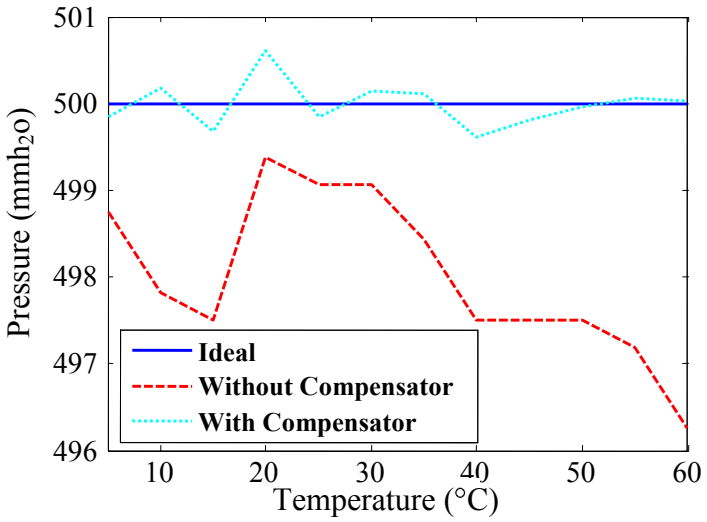

Figure 18. Comaprison between computed input differential pressure of the uncompensated and compensated ATP3100 for the fixed input differential pressure of 500 mmh_2o versus different environment temperatures

These last two figures present that the compensated outputs are nearly temperature invariant and linear. Table 1 also compares the results, without and with the proposed MLP-based compensator in different temperature and input differential pressure, where the impact of the proposed compensated is clearly evident.

Table 1. The ideal, measured, and real input and output values for ATP3100 pressure sensor, without and with the proposed trained MLP-based compensator, in different temperatures and pressures.

Temp.	Ideal Output Current	Ideal Input Pressure	Measured Output Current	Real Computed Pressure	Compensated Output Current	Compensated Computed Pressure
5	8.8	150	8.7900	149.6875	8.8001	150.0029
5	15.2	350	15.1900	349.6875	15.2026	350.0817
10	8.8	150	8.7300	147.8125	8.7972	149.9137
10	15.2	350	15.1200	347.5000	15.1861	349.5669
15	8.8	150	8.7200	147.5000	8.7938	149.8054
15	15.2	350	15.1300	347.8125	15.2009	350.0288
20	8.8	150	8.7600	148.7500	8.8099	150.3079
20	15.2	350	15.1700	349.0625	15.2151	350.4708
25	8.8	150	8.7500	148.4375	8.7869	149.5903
25	15.2	350	15.1700	349.0625	15.1987	349.9608
30	8.8	150	8.7500	148.4375	8.8027	150.0839
30	15.2	350	15.1500	348.4375	15.1887	349.6460
35	8.8	150	8.7200	147.5000	8.8039	150.1230
35	15.2	350	15.1400	348.1250	15.2018	350.0550
40	8.8	150	8.6900	146.5625	8.8016	150.0504
40	15.2	350	15.1200	347.5000	15.2009	350.0291
45	8.8	150	8.6900	146.5625	8.8172	150.5380
45	15.2	350	15.1100	347.1875	15.1999	349.9976
50	8.8	150	8.6700	145.9375	8.8039	150.1204
50	15.2	350	15.1000	346.8750	15.1936	349.8011
55	8.8	150	8.6600	145.6250	8.8028	150.0885
55	15.2	350	15.1000	346.8750	15.2032	350.1001
60	8.8	150	8.6200	144.3750	8.7901	149.6913
60	15.2	350	15.0600	345.6250	15.1928	349.7756

d. Comparing the Results with Other Methods

Table 2 briefly compares the results of the proposed MLP-based compensator with some other similar ANN-based compensators, for different pressure sensors. The pressure measurement error of Patra et al. [4] for CPS is better than 1% FS in a wide temperature range of −20 ~ 70

°C. Futane et al. [8] could achieve the pressure measurement error for Silicon Piezoresistive micro-machined pressure sensor about 1% FS in a less temperature range of 0 ~ 70 °C. Then, Zhou et al. [8] could improve temperature range to −40 ~ 85 °C, with the pressure measurement error to better 0.13% FS. Our proposed method achieves the pressure measurement error to about 0.1% FS for a CPS, which is the best one in the compared methods, while the reported temperature range is 5 ~ 60 °C which is limited by experimental setup.

Table 2. Comparison of different ANN-based compensators for pressure sensors (PS)

Compensated Methods	Pressure Sensor	Pressure Measurement Error	Temperature Range
Patra et al. (2000) [4]	Capacitive PS	1% FS	−20 ~ 70 °C
Futane et al. (2010) [8] (conventional neuron model)	Silicon Piezoresistive micro-machined PS	1% FS	0 ~ 70 °C
Zhou et al. (2014) [10]	Silicon Piezoresistive PS	0.13 % FS	-40 ~ 85 °C
The proposed method	Capacitive PS	0.1% FS	5 ~ 60 °C

V CONCLUSION

Accurate pressure measuring is very important in some critical applications and industries. On the other hand, the CPS, in which the capacitance of a chamber changes based on the input pressure, the output unfortunately suffers from temperature variation as well as nonlinear effects. This paper introduces a simple but effective compensative framework for the CPS using the MLP neural network. The proposed MLP-based compensator tries to overcome temperature dependencies as well as nonlinear operations of CPS. In order to evaluate the effectiveness of this compensator, the proposed framework is applied for ATP3100 smart capacitive pressure transmitter which uses a patented compensating algorithm. At first step, the necessary datasets by carrying out some experiments on the APT3100 should be collected in order to train and test the MLP. After evaluating different MLPs, the proposed MLP which

is a three layer, two inputs, 6 neurons in the first hidden layer, 4 neurons in the second hidden layer, and one output is selected as the best ones. Our simulations in different conditions show that the trained MLP-based compensator by LM algorithm could effectively compensate the output against variation of temperature as well as nonlinear effects. It also improves the pressure measurement error to better than 0.1% FS for the reported temperature range of 5 ~ 60 °C which is not a wide range and it is limited by experimental setup limitations. In future, the proposed compensator should be evaluated in larger temperature ranges.

REFERENCES

[1] Q. Hayat, F. Li-Yun, X.-Zh. Ma and T. Bingqi, "Comparative Study of Pressure Wave Mathematical Models for HP Fuel Pipeline of CEUP at Various Operating Conditions", International Journal of Smart Sensing and Intelligent Systems. Vol. 6, No. 3, pp. 1077-1101, June 2013.

[2] Y. Tao, Zh. Chong, W. Huanming, W. Qisong, Y. Haigang, "A 97 dB dynamic range CSA-based readout circuit with analog temperature compensation for MEMS capacitive sensors", Journal of Semiconductors, Vol. 34, No. 11, pp. (115005)1-8, November 2013.

[3] X. Li, G. Meijer, "An accurate interface for capacitive sensor", IEEE Transaction on Instrumentation and Measurement, Vol. 51, No. 5, pp. 935-939, October 2002.

[4] J.C. Patra, A.C. Kot, G. Panda, "An Intelligent Pressure Sensor using Neural Networks", IEEE Transaction on Instrumentation and Measurement, Vol. 49, No. 4, pp. 829-834, 2000.

[5] C. Pramanic, T. Islam, H. Saha, "Temperature Compensation of Piezoresistive Micro-machined Porous Silicon Pressure Sensor by ANN", Microelectronics and Reliability, Vol. 46, No. 2-4, pp. 343-352, February-April 2006.

[6] Z. Dibi, M.L. Hafiane, "Artificial neural network based hysteresis estimation of capacitive pressure sensor", Physical Status Solid (b), Vol. 244, No. 1, pp. 468-473, 2007.

[7] M. Hashemi, J. Ghaisari, Y. Zakeri, "Modeling and Compensation for Capacitive Pressure Sensor by RBF Neural Networks", 8th IEEE International Conference on Control and Automation, Xiamen, China, June 9-11, pp. 1109-1114, 2010.

[8] N. Futane, S.R. Chowdhury, C.R. Chowdhury, H. Saha, "ANN based CMOS ASIC Design for Improved Temperature-drift Compensation of Piezoresistive Micro-machined

High Resolution Pressure Sensor", Microelectronics and Reliability, Vol. 50, No. 2, pp. 282-291, 2010.

[9] N.P. Futane, S. RoyChowdhury, C. RoyChaudhuri, H. Saha, "Analog ASIC for Improved Temperature Drift Compensation of a High Sensitive Porous Silicon Pressure Sensor", Analog Integrated Circuits and Signal Processing, Vol. 68, No. 3, pp. 383-393, 2011.

[10] M. Hashemi, J. Ghaisari, A. Salighehdar, "Identification and Compensation of a Capacitive Differential Pressure Sensor Based on Support Vector Regression Using Particle Swarm Optimization", Intelligent Automation & Soft Computing, Vol. 18, No. 3, pp. 263-277, 2012.

[11] G. Zhou, Y. Zhao, F. Guo, W. Xu, "A Smart High Accuracy Silicon Piezoresistive Pressure Sensor Temperature Compensation System", Sensors, Vol. 14, No. 7, pp. 12174-12190, 2014.

[12] J. Qi，J. Cai, "Error Modelling and Compensation of 3D Scanning Robot System based on PSO-RBFNN", International Journal of Smart Sensing and Intelligent Systems, Vol. 7, No. 2, pp. 837-855, June 2014.

[13] P. Moallem, A. Monadjemi, "An Efficient MLP Learning Algorithm using Parallel Tangent Gradient and Improved Adaptive Learning Rates", Connection Science, Vol. 22, No. 4, pp. 373-392, December 2010.

[14] S.C.Mukhopadhyay, "Quality inspection of electroplated materials using planar type micro-magnetic sensors with post processing from neural network model", IEE Proceedings – Science, Measurement and Technology, Vol. 149, No. 4, pp. 165-171, July 2002.

[15] S.C.Mukhopadhyay, S.Yamada and M.Iwahara, "Evaluation of near-surface material properties using planar type mesh coils with post-processing from neural network model", International journal Studies in Applied Electromagnetics and Mechanics, IOS Press Vol. 23, pp. 181-189, 2002.

[16] APT3100 Smart Pressure Transmitter Operation Manual, http:// www.autroltransmitters.com

[17] S. Samarasinghe, Neural Networks for Applied Sciences and Engineering: From Fundamentals to Complex Pattern Recognition, Auerbach Publications, New York, 2006.